A STUDY OF SEDIMENT MIXING IN SURF AND SWASH ZONES UNDER ACCRETIONAL AND EROSIONAL WAVE CONDITIONS

Thamali Gunaratna[1], Takeshi Kurosaki[2] and Takayuki Suzuki[3]

Abstract

Two-dimensional flume-test experiments were conducted to investigate the temporal and spatial sediment movement and mixing depths from the offshore side of the surf zone to the swash zone. Three colored fluorescent-sand tracers were installed on the bed surface at three locations. Six core samples were collected at different cross-shore locations covering the concerned areas at 10 min intervals. The tracer particles in each core sample along the depth were counted. The experiments could represent the sediment-mixing depths with respect to time for the concerned areas under accretion and erosion. A berm was created in the first 30 min of deposition, which was washed away by erosional waves. The offshore-placed tracer appeared largely on the surface layers whereas the other colors were mixed for depths of up to a maximum of 3 cm from the initial profile. The maximum-mixing depths were observed near the wave-breaking region.

Key words: laboratory experiment, tracer study, cross-shore sediment transport, core sampling, berm, wave break point

1. Introduction

Sediment transport is highly dynamic around the boundary regions that connect the land and ocean. It undergoes continuous topography changes temporally and spatially. The hydrodynamic forces acting on the seabed profile lead to beach erosion and accretion, which have grabbed the attention of many researches. Beach erosion is currently observed in many parts of the world, affecting natural habitats as well as human beings (Feagin et al., 2005). This type of erosion is due to man-made structures, beach mining (Cooper and Pethick, 2005), and severe weather conditions (Douglass, 1994). Eighty percent of the world's population lives within a radius of 1 km from the coastline (Blinovskaya, 2012). In the United States alone, it is estimated that 80–90% of the beaches may undergo erosion, which can directly affect the economy (Leatherman, 2001). Japan is another country which is prone to erosion. Losing land will directly impact the coast with severe sea conditions it has to face (Isobe, 1998). Beach accretion affects coral growth and nearshore ecosystems, thus significantly influencing the structure, biomass, and metabolism of seabed habitats (Airoldi et al., 1996).

 Coastal-sediment transport is divided into longshore and cross-shore directions based on different coastal processes. The longshore-sediment transport due to longshore currents and angled waves leads to long-term variations in the beach profile (Frihy and Komar, 1993). The effects of wave breaking and turbulence will be manifested in cross-shore transport in a time scale of several seconds to months, seasonally affecting the nearshore bed profile (Dean and Dalrymple, 2004). Among the different coastal processes, the sediment transport is one of the most complicated natural phenomena, on which considerable amount of research is conducted; nevertheless, the studies need to be improved. Until now, many empirical equations have been developed to estimate the sediment movement. Currently, several numerical models are being implemented to obtain precise and reasonable results. Owing to the extensive amount of field data required for calibration and validation purposes, using numerical models in morphological studies is quite challenging (Vousdoukas et al., 2012). Apart from the numerical approaches, the experimental approaches of evaluating the behavior of nearshore-sediment transport have a vast historical base.

[1]Graduate School of Urban Innovation, Yokohama National University, Japan. gunaratna-menaka-gz@ynu.jp
[2]Graduate School of Urban Innovation, Yokohama National University, Japan. kurosaki-takeshi-mb@ynu.jp
[3]Faculty of Urban Innovation, Civil Eng. Dept., Yokohama National University, Japan. suzuki-t@ynu.ac.jp

Sediment mixing near the surf zone is a result of wave breaking, nearshore currents, and winds (Airoldi et al., 1996). The natural phenomenon of nearshore-sediment mixing is analyzed via the mixing depths obtained in several experimental studies conducted on tracers in the past. Some of the tracers used were color-coated sediment particles, radionuclides, and mineral soil (Feagin et al., 2005). The studies conducted on mixing and movement of nearshore sediments are employed in the studies pertaining to coral and shell growth, beach nourishment, and other ecosystems. Fluorescent-sand experiments have been conducted to analyze the concepts of sediment mixing, longshore-sediment transport (Inman et al., 1971; Katoh and Tanaka, 1986; Smith et al., 2007; Bellido et al., 2011;), and cross-shore sediment transport (Kraus et al., 1993; Otsuka and Watanabe, 2014; Suzuki et al., 2017). In addition to the effect of wave heights, the effects of beach-slope variations (Bertin et al., 2007) and longshore-current velocities are considered. Many definitions were introduced to define the sediment-mixing depth in past case studies. The depth of 80% of the particles to be found and the centroids or the weighted average of tracer advected depths are some of the commonly used definitions. Each definition has concluded a linear relationship of mixing depths, b, with the wave breaking heights, H_b, or significant wave heights, $H_{1/3}$ ($b = 0.08H_{1/3}$ by Nadaoka et al., 1981; $b = 0.027H_b$ by Kraus et al., 1982; $b = 0.1H_{1/3}$ by Katoh and Tanaka, 1986). However, most of the past studies were limited to the area in the swash zone or in the surf zone.

The objective of this study is to analyze the spatial and temporal variations in the cross-shore sediment movement in the nearshore, from the swash zone to the offshore side of the surf zone under erosional and accretional-wave conditions. The bed-profile variation with respect to time, quantitative values of the fluorescent particles in the cross-shore profile and depth, and temporal and spatial variations in the mixing depth are obtained from laboratory experiments. Moreover, the sediment-mixing depths along the cross shore are discussed.

2. Methodology

The laboratory experiments were conducted in a glass-walled flume at Yokohama National University. The length, width, and height of the flume are 18.0 m, 0.50 m, and 0.50 m, respectively. Fine sand was filled for an impermeable 1/20 bed slope of the flume with $d_{50} = 0.2$ mm, up to a thickness of 5.0 cm. Figure 1 shows the experimental setup of the bed profile and installation of wave gauges. Two wave gauges were installed to record the water-surface motions along the offshore and edge of the slope. In the experiments, the origin of the cross-shore distance was set at the edge of the slope. The x and z axes represented the onshore and upward directions, respectively. Fluorescent-sand tracers of blue, yellow, and red colors were horizontally placed on top of the bed layer with a mass of 6 g at each fixed cross-shore location, $x = 2.05$ m, 3.15 m, and 3.7 m, respectively (Figures 1 and 2). The offshore water depth was set as 26.0 cm. Two regular wave conditions were used in this study: accretional and erosional-wave conditions.

In the experiments, the initial sand-bed condition was set as flat with a slope of 1/20. The accretion case of waves, a wave height of 1.8 cm, and a wave period of 2.0 s were generated for 30 min. In this case, a berm was formed in the swash zone. After the accretion scenario, the erosional case of waves, a wave height of 2.8 cm, and a wave period of 8.0 s were generated for 20 min. The berm was completely eroded by the erosional waves. The two wave conditions were determined via a trial-and-error method such that the berm shape is formed and is eroded under each wave condition.

During the experiments, the bed-profile survey and sand-core samplings were conducted every 10 min. At each 10-min interval during the accretional and erosional-wave conditions, the wave generator was stopped and the water level was lowered until approximately $h = 16$ cm to remove the core samples and conduct the bed-profile survey. After removing the core samples and conducting the profile survey, the water was refilled until $h = 26.0$ cm for the next experiment. The longshore direction of the investigated area was divided into five sections, each with a width of 10 cm. To avoid unexpected sediment mixing due to core sampling, each time step of the core sampling was conducted in different sections. At each core sampling, six cores were placed at fixed cross-shore locations; *i.e.*, $x = 2.05$ m, 2.75 m, 3.15 m, 3.45 m, 3.7 m, and 3.85 m (Figure 1). The core-sampling positions were determined from the trial runs wherein the bed profile changed significantly from the initial profile. A PVC tube with a length of 12.0 cm and a diameter of 3.0 cm was used for the core sampling (Figure 3a).
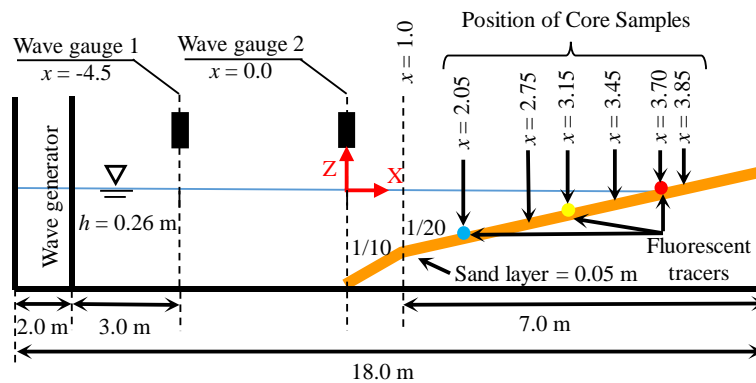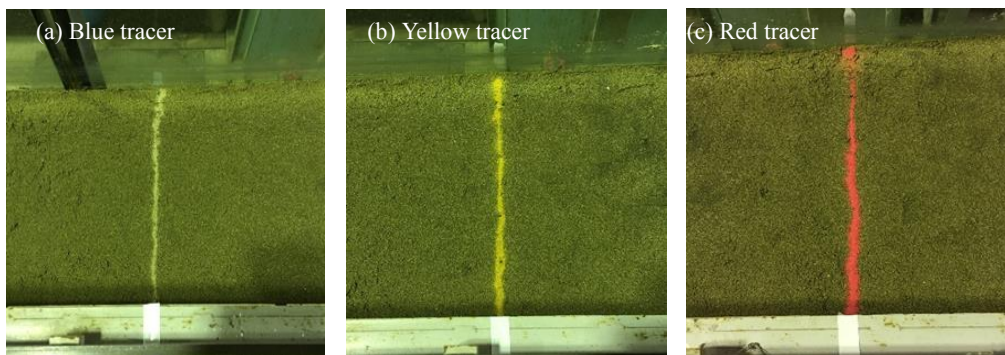
Figure 1. Experimental setup

Figure 2. Fluorescent-sand tracer strips placed across the flume width; (a) x = 2.05 m for blue, (b) x = 3.15 m for yellow, and (c) x = 3.70 m for red.
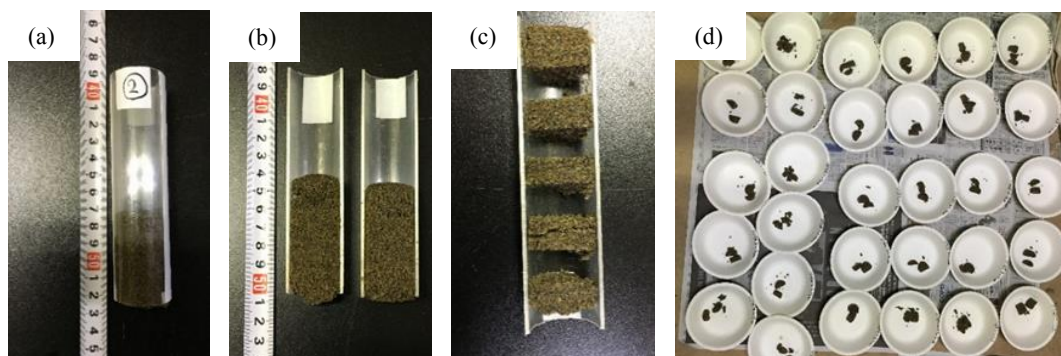

Figure 3. Dividing procedure of each core; (a) Sampled core, (b) Split into half, (c) Dividing the sample, and (d) Air dried.

After collecting the cores, the tubes were split into half and divided into 1-cm sand-layer samples (Figures 3b and 3c). Each sand-layer sample was air dried (Figure 3d), and subsequently, transferred into a dark room to count the number of fluorescent-sand tracers of each color using a UV light source.

Several definitions are proposed for the mixing depths: Katoh and Tanaka (1986) suggested a core depth of 80% of a tracer has reached, and the centroids or the weighted average depths where a tracer has reached (Kraus et al., 1982). In the preliminary core-sampling test, fewer than 10 particles were found in the middle layer of a divided sample, though the tracers were spread only on the bed surface. Thus, in this experiment, the mixing depth was defined as the depth where more than 10 tracers were found except in the top-surface layer, wherein the sampling errors were considered minimum.

3. Results and Discussions

3.1 *Bed-profile changes and temporal-spatial distributions of fluorescent-sand tracers*

Figures 4a and 4b show the bed-profile changes during the experiments conducted under the accretional and erosional conditions, respectively. The time t is the total time from the start time of the accretion case. Under both the wave conditions, the bed profile significantly changes from the initial condition. The bed profiles where the yellow and red tracers were installed, i.e., $x = 3.15$ m and $x = 3.70$ m, respectively, fluctuated under the accretional and erosional conditions. However, the position at which the blue tracer was installed, i.e., $x = 2.05$ m, remained largely constant with respect to time.
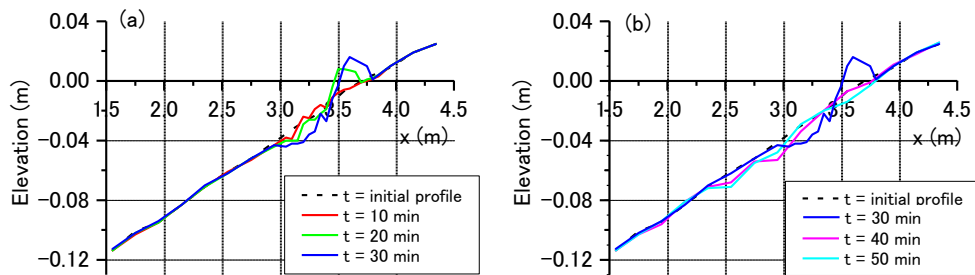

Figure 4. Variation in bed profile; (a) Accretion case, and (b) Erosion case.

In the accretion case, the variation in the bed profile indicates that the berm shape was created with a height of 2 cm near the shoreline at $x = 3.7$ m (Figure 4a). In this case, the breaking point of the wave was at approximately $x = 3.25$ m. The figure shows that the height of the berm increases and shifts toward the onshore side with the passage of time. In contrast, the area from $x = 2.9$ m to 3.4 m of the bed profile eroded during the berm formation.

After the berm was formed, the erosional waves were generated (from $t = 30$ min to 50 min). As the wave period was long in this case, the distance between the wave run-up and run-down points was considerable. The wave started to break at approximately $x = 3.3$ m. The berm started to disappear within the first 2 min of the experiment. After generating the erosional waves for 10 min, i.e., $t = 40$ min, the berm was completely eroded, and the bed profile largely returned to the initial profile levels (Figure 4b). After generating the erosional waves for 20 min, i.e., $t = 50$ min, the eroded profile was observed at the offshore side of the breaking point. In the erosion case, the wider area of the bed profile, from approximately $x = 2.25$ m to $x = 4.0$ m, was disturbed by the waves.

Figures 5–9 show the cross-shore and vertical distributions of the fluorescent-sand tracers for blue, yellow, and red at each time step. The vertical axis represents the elevation. The origin was set as the initial bed-profile level at each location. The solid lines in the figures indicate the bed level of each time step, shown in the title of the figures. The dashed lines indicate the bed level of the previous time step, i.e., the bed level before 10 min. The bar charts represent the total number of tracers at each layer. The tracer counts below 10 were removed from the results, except the ones at the top of the layer. The number of counts in the bar chart reached up to 100, indicating that more than 100 particles were found in the layer.

After the first 10 min of the experiment, as shown in Figure 5 (accretion case), the blue tracers installed at $x = 2.05$ m (Figure 5a) were found only on the surface layer at the offshore region. Although the tracers were installed at the location, as shown in Figure 5a, only a few were collected at nearby locations. The yellow tracers installed at $x = 3.15$ m (Figure 5c) were largely found at the installed location; moreover, the tracers were mixed along the depth without changing the bed profile, particularly around the impinging point. The results show that the sediment mixed before the change in topography. The red tracers installed at $x = 3.70$ m (Figure 5e) were transported toward both onshore and offshore sides. After 20 min from the beginning, as shown in Figure 6, most of the blue tracers were transported to the area near $x = 2.75$ m. Few blue tracers were found on the surface of the onshore side from $x = 3.15$ m. The core-sample location at $x = 3.15$ m decreases in profile depth up to 1 cm; the location increased at $x = 3.45$ m by 1 cm. The maximum number of colored tracers were collected at the location $x = 3.45$ m. At the end of the accretion case, i.e., $t = 30$ min, the yellow tracers were transported more toward the onshore side, and the maximum number of

blue tracers was found again at $x = 2.75$ m, as shown in Figure 7. The red tracer mixed more along the depth at $x = 3.70$.
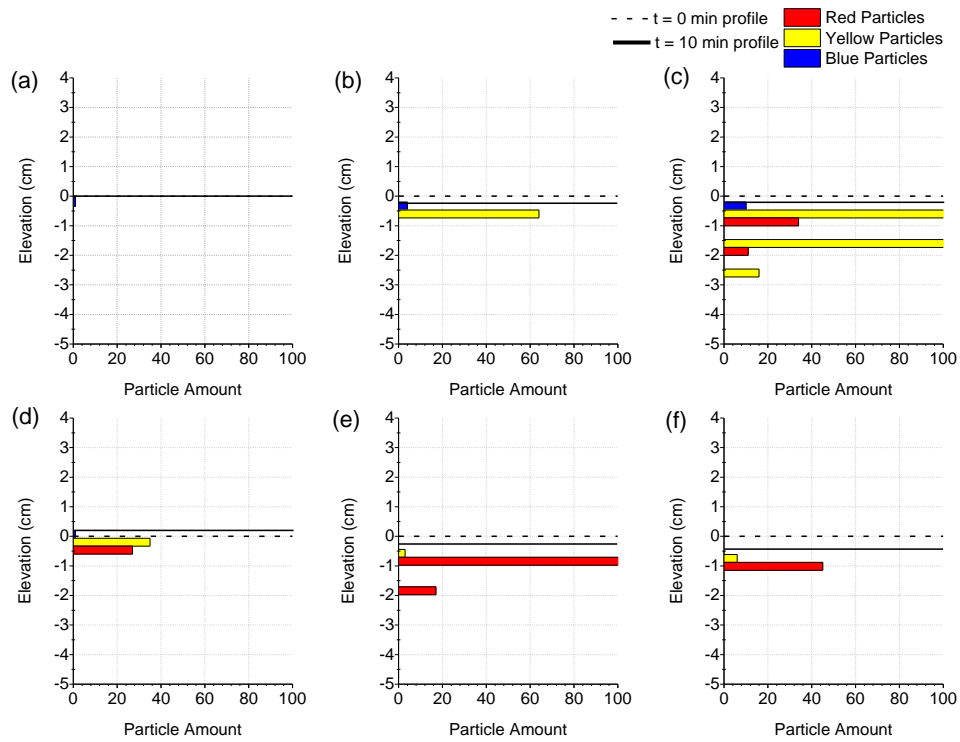

Figure 5. Number of tracer particles along the depth after 10 min at each location under accretion condition; (a) $x = 2.05$ m, (b) $x = 2.75$ m, (c) $x = 3.15$ m, (d) $x = 3.45$ m, (e) $x = 3.70$ m, and (f) $x = 3.85$ m.
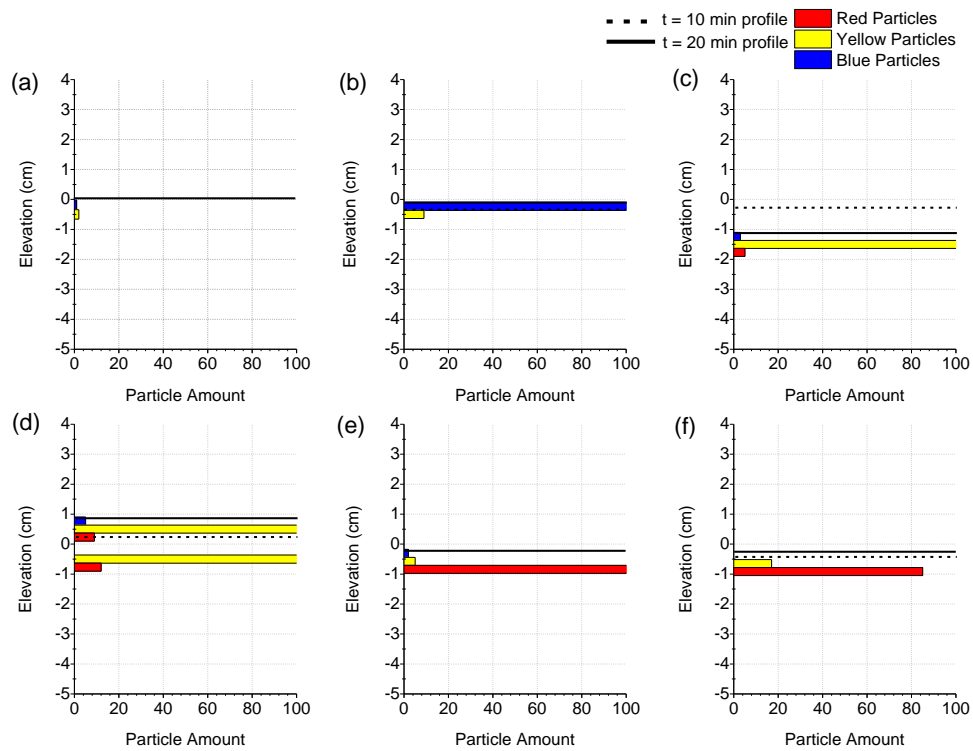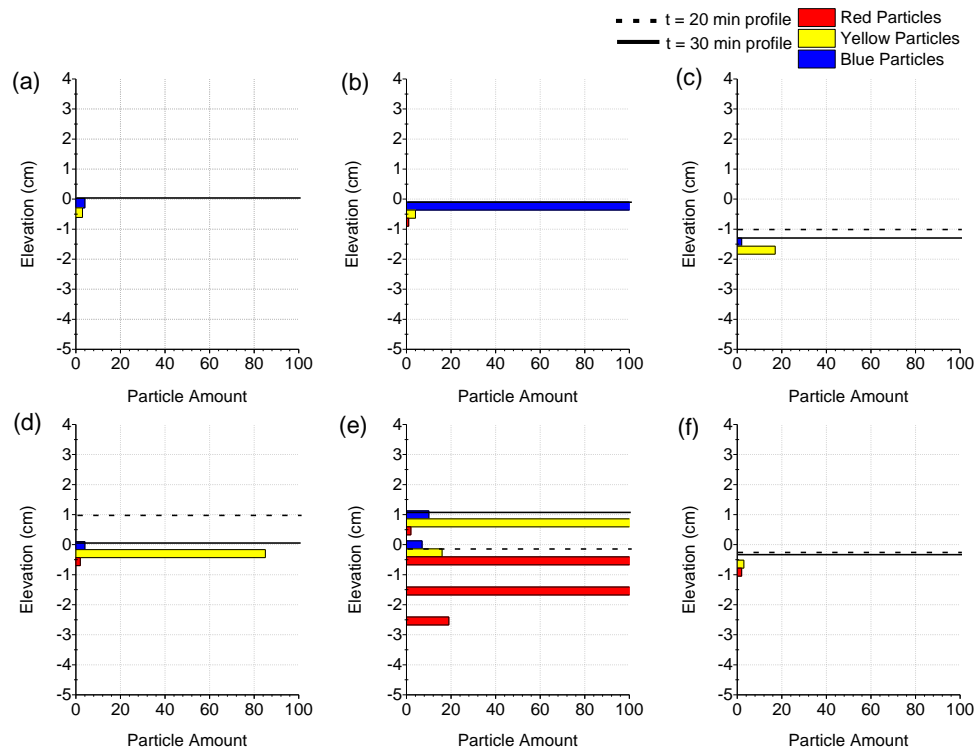

Figure 6. Number of tracer particles along the depth after 20 min at each location under accretion condition; (a) $x = 2.05$ m, (b) $x = 2.75$ m, (c) $x = 3.15$ m, (d) $x = 3.45$ m, (e) $x = 3.70$ m, and (f) $x = 3.85$ m.
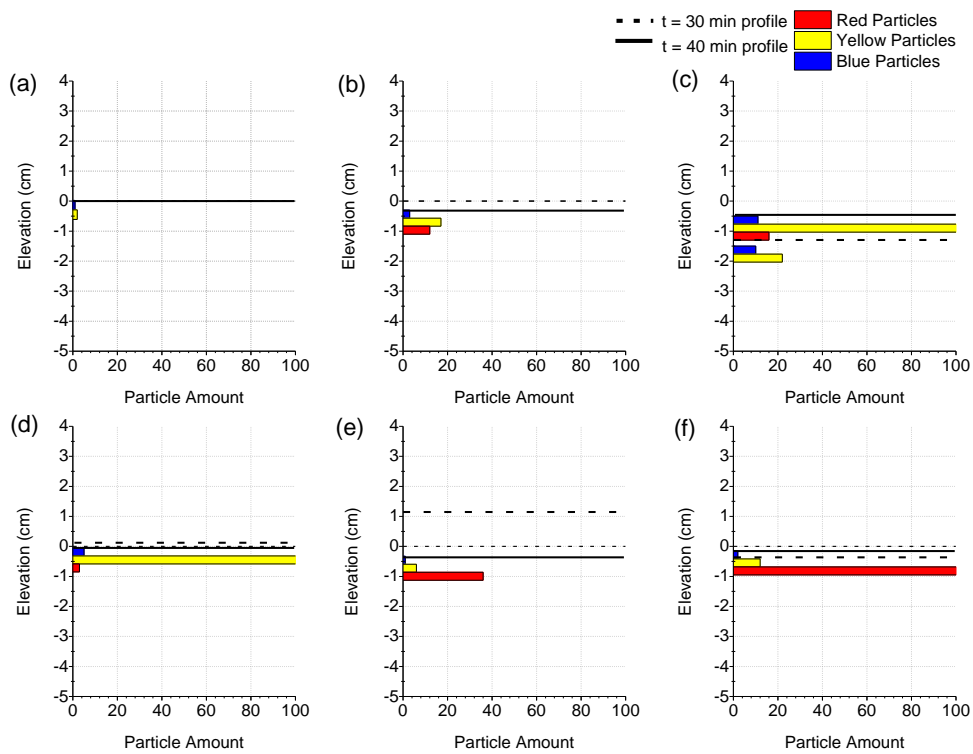
Figure 7. Number of tracer particles along the depth after 30 min at each location under accretion condition; (a) *x* = 2.05 m, (b) *x* = 2.75 m, (c) *x* = 3.15 m, (d) *x* = 3.45 m, (e) *x* = 3.70 m, and (f) *x* = 3.85 m.

Figure 8. Number of tracer particles along the depth after 40 min at each location under erosion condition; (a) *x* = 2.05 m, (b) *x* = 2.75 m, (c) *x* = 3.15 m, (d) *x* = 3.45 m, (e) *x* = 3.70 m, and (f) *x* = 3.85 m.
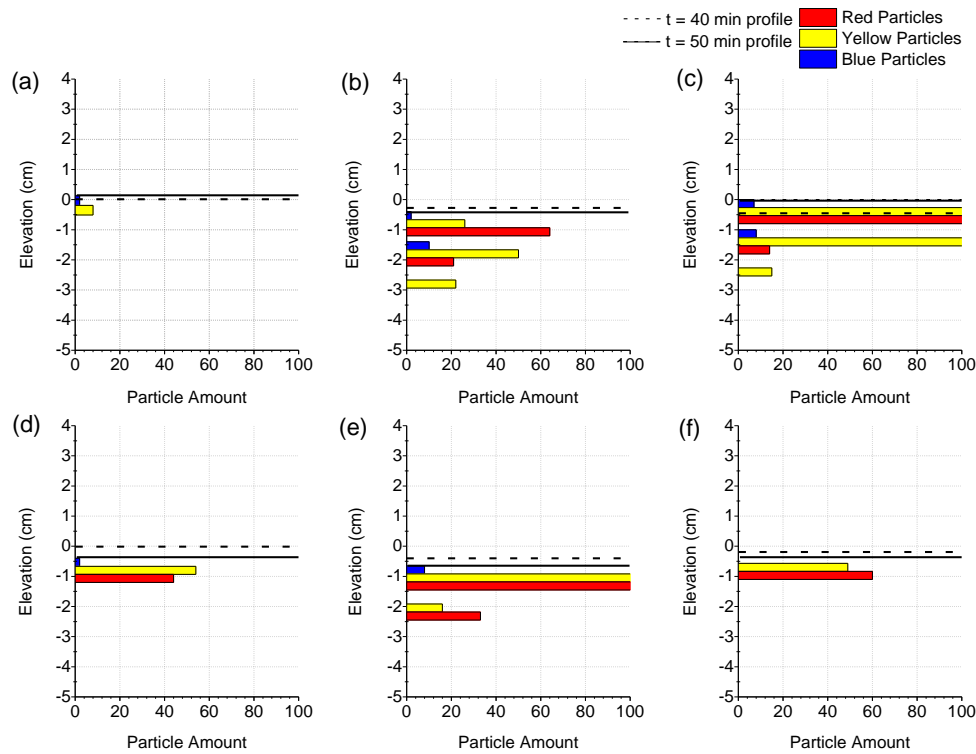
Figure 9. Number of tracer particles along the depth after 50 min at each location under erosion condition; (a) *x* = 2.05 m, (b) *x* = 2.75 m, (c) *x* = 3.15 m, (d) *x* = 3.45 m, (e) *x* = 3.70 m, and (f) *x* = 3.85 m.

The bed profile starts decreasing more than 1 cm at *x* = 3.15 m; however, the profile increases by 1 cm at *x* = 3.7 m. The highest number of tracer-gathering point shifts toward the onshore location *x* = 3.7 m. Until the end of accretional waves, the blue tracers significantly remained at the same location, *i.e.*, *x* = 2.75 m. The yellow and red tracers mixed well on the surface and along the depth at all locations except for the most offshore sampling location, i.e., *x* = 2.05 m. The position of highest number of all colors collected along the depth was initially recorded at *x* = 3.15 m; this position shifted with the progress of time until *x* = 3.45 m.

In the beginning of the erosional-wave conditions (after 40 min from the start of the experiment, *i.e.*, *t* = 40 min, as shown in Figure 8), most of the blue tracers were washed away, which collects at *x* = 2.75 m in the previous interval. More number of yellow tracers were collected at *x* = 3.15 m and 3.45 m whereas more number of red tracers were located at *x* = 3.7 m and *x* = 3.85 m. A slight decrease in the bed profile was observed at *x* = 2.75 m, 3.15 m, and 3.7 m. In this time step, the maximum number of colored tracers was mixed at *x* = 3.15 m up to a depth of 2 cm.

At the end of the erosional wave conditions, *i.e.*, *t* = 50 min, as shown in Figure 9, the red and yellow tracers were mixed along the depth at higher concentrations whereas the blue tracers appeared only at several locations in the surface layers. The highest mixing depth was reached at *x* = 2.75 m. The highest quantities of tracers was collected at *x* = 3.15 m.

3.2 *Temporal and spatial distributions of mixing depth*

Using the results obtained from the tracer experiments, the temporal and spatial distributions of the mixing depth were analyzed. Figure 10 shows the temporal and spatial distributions of the mixing depth for the blue tracers. In the panel (a), a thick solid line indicates the surface profile at each time step. The blue tracers were installed at the most offshore location near the offshore side of the surf zone, *i.e.*, *x* = 2.05 m. The maximum mixing depth during the accretion and erosion cases were 1 cm and 2 cm, respectively. In the accretion waves, the tracers mixed along the depth at the wave-breaking point, *i.e.*, *x* = 3.20 m. Although the bed profile changed, the mixing depths of the blue tracers remained constant from the

offshore zone to the swash zone. Under the erosional-wave conditions, a higher mixing depth was observed at $x = 2.75$ m, which was the offshore side of the wave-breaking point. The overall sediment movement was toward the onshore direction in the accretion case and toward the offshore direction in the erosion case in the experiment.
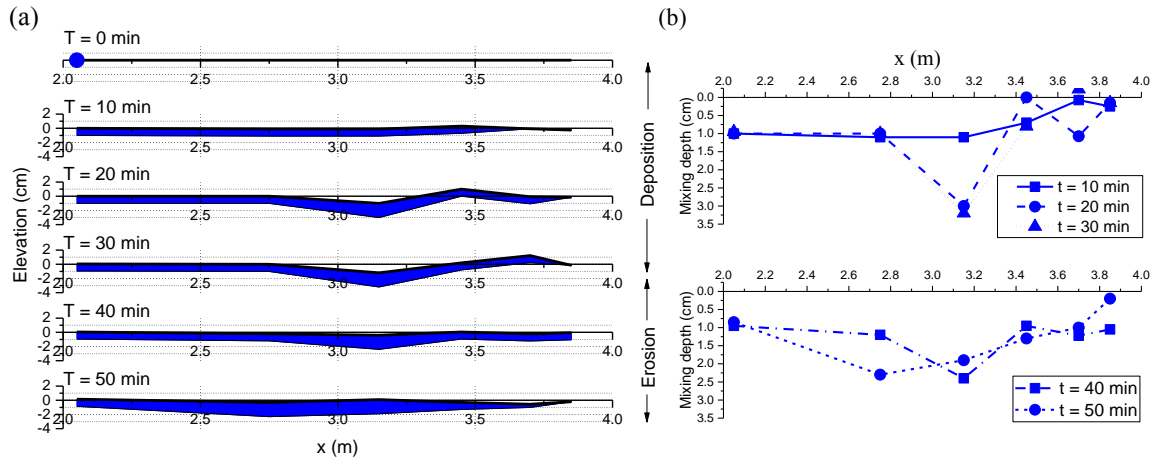

Figure 10. Mixing depth of blue tracers; (a) Temporal and spatial distributions of mixing depth, (b) Mixing depths from the bed surface level of each time step.
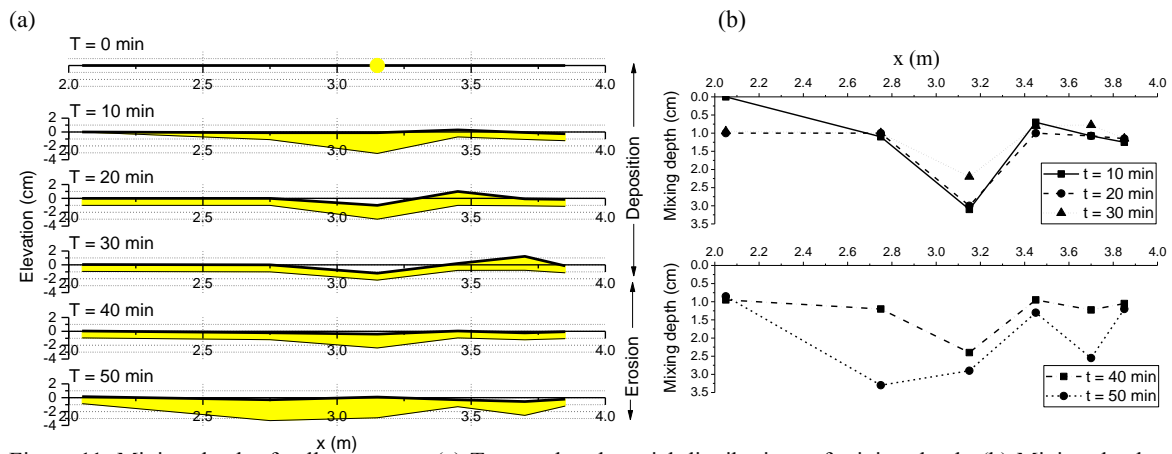

Figure 11. Mixing depth of yellow tracers; (a) Temporal and spatial distributions of mixing depth, (b) Mixing depths from the bed surface level of each time step.
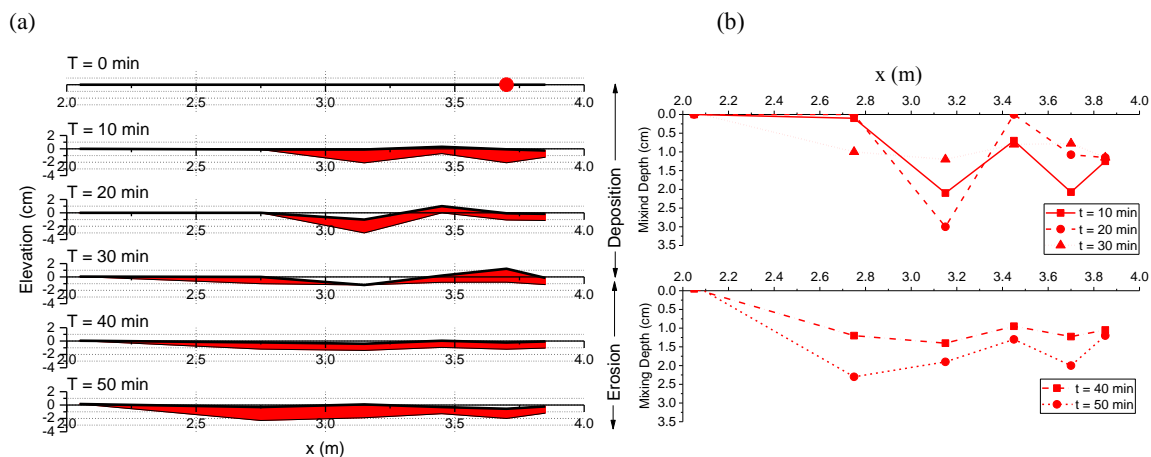

Figure 12. Mixing depth of red tracers; (a) Temporal and spatial distributions of mixing depth, (b) Mixing depths from the bed surface level of each time step.

Figure 11 shows the temporal and spatial distributions of the mixing depth for the yellow tracers. The yellow tracers were installed in the wave-breaking area, *i.e.*, $x = 3.15$ m. The maximum mixing depth for the accretion and erosion cases was 3 cm. The mixing depths varied with respect to time and space continuously throughout the surf zone. In the beginning of the experiment, *i.e.*, 10 min, the bed profile was largely constant, and the mixing depth around the breaking point reached up to 3.0 cm. After the mixing, the profile changed, and the berm started to form in the swash zone.

Figure 12 shows the temporal and spatial distributions of the mixing depth for the red tracers. The red tracers were installed near the swash zone, *i.e.*, $x = 3.70$ m. During the first 20 min, the tracers were mixed only till the offshore side at $x = 2.75$ m. The sediments in the swash zone moved to the offshore side owing to the back wash and under tow. The sediment mixing occurred because of wave breaking and bore effects. Under the erosional-wave conditions, the red tracers were transported toward the offshore direction.

4. Conclusion

Laboratory flume experiments were conducted to investigate the sediment movement in the cross-shore direction with respect to time from the offshore side of the surf zone to the swash zone. Three colored fluorescent-sand tracers were placed at three different cross-shore locations: offshore side of the surf zone, wave-breaking area, and near the shoreline. During the experiments, the bed-profile observations and core sample collections were conducted at six different cross-shore locations with an interval of 10 min. The berm was created during the first 30 min by the accretional waves and was eroded in the next 20 min by the erosional waves. At 10-min intervals, the sediment mixing patterns were analyzed.

Although the variation in the bed profile is constant, the mixing depths were measured from the initial bed profile (1/20 flat slope) arranged prior to conducting the experiments. A dynamic pattern of sediment mixing occurred in the wave-breaking zones in the swash-zone direction. The highest mixing-depth location shifted to the nearby sampling location at each 10-min interval toward the shore direction during the accretional waves and toward the offshore direction under the erosional waves. The highest number of tracer colors was recorded at the maximum mixing-depth position at each interval.

The mixing depths and sediment movement were observed to be a combined effect of wave breaking, wave intensity, experiment duration, etc. The correlation between the mixing depths and hydrodynamic forces can be analyzed using the numerical results. The depth of disturbance (or the mixing depth) from the wave breaking and turbulence created nearshore is significant from the offshore side of the surf zone to the swash zone. The nearshore dynamics should be further studied to understand this complex scenario.

References

Airoldi, L., Fabiano, M. and Cinelli, F., 1996. Sediment deposition and movement over a turf assemblage in a shallow rocky coastal area of the Ligurian Sea. *Marine Ecology Progress Series*, 133, 241-251.
Bellido, C., Anfuso, G., Plomaritis, T.A. and Buitrago, N.R., 2011. Morphodynamic behaviour, disturbance depth and longshore transport at Camposoto Beach (Cadiz, SW Spain). *Journal of Coastal Research*, 64, 35.
Bertin, X., Deshouilieres, A., Allard, J. and Chaumillon, E., 2007. A new fluorescent tracers experiment improves understanding of sediment dynamics along the Arcay Sandspit (France), *Geo-Marine Letters*, 27(1), 63-69.
Blinovskaya, Y.Y., 2012. Topical Coastal Environmental Issues of Japan Sea. *Shimane Journal of North East Asian Research*, 23, 41-46.
Cooper, N. J. and Pethick, J. S., 2005. Sediment budget approach to addressing coastal erosion problems in St. Ouen's Bay, Jersey, Channel Islands. *Journal of Coastal Research*, 112-122.
Dean, R. G. and Dalrymple, R. A., 2004. *Coastal processes with engineering applications*. Cambridge University Press.

Douglass, S. L., 1994. Beach Erosion and Deposition on Dauphin Island, Alabama, U.S.A. *Journal of Coastal Research,* 10(2), 306-328.

Feagin, R. A., Sherman, D. J. and Grant, W. E., 2005. Coastal erosion, global sea-level rise, and the loss of sand dune plant habitats, *Frontiers in Ecology and the Environment*, 3, 359–364.

Frihy, O. E. and Komar, P. D., 1993. Long-term shoreline changes and the concentration of heavy minerals in beach sands of the Nile Delta, Egypt. *Marine Geology*, 115(3-4), 253-261.

Inman, D. L., Tait, R. J. and Nordstrom, C. E., 1971. Mixing in the surf zone. *Journal of Geophysical Research*, 76(15), 3493-3514.

Isobe, M., 1998, July. Toward integrated coastal zone management in Japan. In *ESENA Workshop: Energy-Related Marine Issues in the Sea of Japan*, 11-12.

Katoh, K. and Tanaka, N., 1986. Local movements of sand in the surf zone. *Coastal Engineering Proceedings*, 1(20).

Kraus, N. C., Isobe, M., Igarashi, H., Sasaki, T. O. and Horikawa, K., 1982. Field experiments on longshore sand transport in the surf zone. *Coastal Engineering*, 969-988.

Kraus, N. C., Jane M. S. and Charles K. S., 1993. SUPERTANK laboratory data collection project. *Coastal Engineering 1992*. 2191-2204.

Leatherman, S. P., 2001. Social and economic costs of sea level rise. *International Geophysics*, 75, 181-223.

Nadaoka, K., Tanaka, N. and Katoh, K., 1981. Field observation of local sand movements in the surf zone using fluorescent sand tracer. *Port and Harbour Research Institute*, 20(2), 75-126.

Otsuka, J. and Watanabe, Y., 2014. Laboratory measurement of sediment transport under a breaking wave turbulent flow field, *Coastal Engineering Proceedings*, 1(34), 2.

Smith, S.J., Marsh, J. and Puckette, T., 2007. Analysis of Fluorescent Sediment Tracer for Evaluating Nearshore Placement of Dredged Material. In *Proceedings XVIII World Dredging Congress 2007*.

Suzuki, T., Inami, Y., Banno, M. and Kuriyama, Y., 2017, Observation of sediment particle movements during a storm, *Coastal Dynamics 2017*, In press.

Vousdoukas, M. I., Ferreira, Ó., Almeida, L. P. and Pacheco, A., 2012. Toward reliable storm-hazard forecasts: XBeach calibration and its potential application in an operational early-warning system. *Ocean Dynamics*, 62(7), 1001-1015.